Polímeros
ISSN 1678-5169 (Online)

https://doi.org/10.1590/0104-1428.20220066

ORIGINAL ARTICLE

In-line rheo-optical characterization of PET hydrolysis and chain extension during extrusion

Luciana Assumpção Bicalho[1] and Sebastião Vicente Canevarolo Junior[2*]

[1]Programa de Pós-graduação em Ciência e Engenharia de Materiais – PPG-CEM, Universidade Federal de São Carlos – UFSCar, São Carlos, SP, Brasil

[2]Departamento de Engenharia de Materiais – DEMa, Universidade Federal de São Carlos – UFSCar, São Carlos, SP, Brasil

**e-mail: caneva@ufscar.br*

Abstract

The thermo-mechanical degradation of PET during extrusion was studied in the transient state. Active agents, water, causing hydrolysis by chain scission and pyromellitic dianhydride PMDA, causing chain extension, were added to the extrusion flow as pulses. They change the PET molecular weight, affecting its the melt flow elasticity, which was followed in-line by a rheo-optical detector set in an instrumented slit-die, measuring synchronously, pressure drop and flow birefringence (Δn_{12}). The effect of the extrusion shearing level, set by 90º kneading blocks with different lengths, was also quantified. The results, as of residence time distribution curves, show the degree of thermo-mechanical degradation as hydrolysis and chain extension for each pulse type and concentration. Thus, assuming collinearity and full birefringence orientation along the melt flow the first normal stress difference N_1 can be monitored in-line.

Keywords: *chain extension, hydrolysis, in-line rheo-optical characterization, polyethylene terephthalate, twin-screw extruder.*

How to cite: Bicalho, L. A., & Canevarolo Junior, S. V. (2023). In-line rheo-optical characterization of PET hydrolysis and chain extension during extrusion. *Polímeros: Ciência e Tecnologia*, *33*(2), e20230016. https://doi.org/10.1590/0104-1428.20220066

1. Introduction

PET during the extrusion process may undergo hydrolytic thermo-mechanical degradation (TMD), decreasing its molecular weight and, consequently, its melt viscosity and mechanical properties. To avoid hydrolysis reaction, the moisture content in PET should be lower than 0.02% w/w before processing takes place[1,2]. When PET hydrolytic degradation occurs, it induces chain scission reactions at ester linkages. Each water molecule breaks down one ester bond, creating a carboxyl and a hydroxyl chain end group, reducing the PET molecular weight[3,4]. Several test methods were proposed to quantify PET hydrolysis[5,6]. Pirzadeh et al.[5] showed that hydrolysis occurs by both moisture and heat rather than an individual effect. Degradation at temperatures lower than its Tg was less prominent but increased above it. Crystallinity degree plays a crucial role in preventing hydrolytic degradation extent. Hosseini et al.[6] exposed fiber PET chips to water at 85°C for different periods, during the first 5 days, degradation co-occurred with the penetration of water molecules. After saturation, degradation continues sustained by water molecules still present in the PET.

The use of chain extenders can partially compensate hydrolytic degradation. In this process, a di- or poly-functional low-molecular weight material is added to react with PET chain end groups, rejoining the broken chains resulting from the PET chain scission during the melting process. Pyromellitic dianhydride PMDA has been reported as an efficient chain extender[1,7,8]. Being poly-functional, it can react with up to four PET end chains, tying them together. Awaja et al.[7] reported that PMDA was an effective chain extender for industrial-scale recycled PET, depending on its concentration. Incarnato et al.[8] used PMDA to increase the industrial PET molecular weight. By using higher concentrations, from 0.50 to 0.75%, PMDA promotes extensive chain extension reactions, making them suitable for film blowing and blow molding processes.

Obtaining real-time quantitative data on hydrolysis and chain extension would simplify quality control by providing fast quantification of the effects of processing conditions, screw geometry, and material formulations[9,10]. Also, rheo-optical techniques have fast response times and do not disturb the analyzed environment.

Birefringence is an attractive optical property, which is present when the polymer shows optical anisotropy, creating difference between two orthogonal refractive indexes. Different types of birefringence may coexist in polymer parts: intrinsic, stress/strain, form, and flow. The flow birefringence, in the way is optically measured here, directly relates the birefringence across the flow (Δn_{13}) and the third normal stress difference ($N_3 = \sigma_{11} - \sigma_{33}$) developed during the polymer extrusion. It follows the Stress-Optical Rule,

SOR, in which C is the stress-optical coefficient, dependent of the chemical structure of the polymer and temperature[11].

$$\Delta n_{13} = n_{11} - n_{33} = CN_3 = C\left(\sigma_{11} - \sigma_{33}\right) \quad (1)$$

In turn the first normal stress difference (N_1), which indicates the material's elasticity related to shear stress, can be written as:

$$\Delta n_{12} = \frac{C}{\cos 2\chi} N_1 = \frac{C}{\cos 2\chi}\left(\sigma_{11} - \sigma_{22}\right) \quad (2)$$

being χ the orientation angle, the angle between the principal directions of the stress tensor and the principal directions of the refractive index tensor, the same as the extinction angle (θ) for the flow birefringence measurements. However, it's difficult to check the validity as there is no direct way of determining σ_{11}-σ_{22}. Work in this respect was carried out in the case of 1-2 plane, polymer solutions and, for slit die[12]. Nevertheless, it has been seen that for polymer melts, the $N_1 \cong N_3$[12], making $N_2 = \sigma_{22} - \sigma_{33} \cong 0$.

This work presents an experimental setup and a method to monitor the third normal stress difference N_3 by quantifying in-line the flow birefringence in the gradient 2-direction (1-3 plane), during melt extrusion. By assuming that the flow birefringence produced is fully oriented and colinear along with the extrusion melt flow one can say that N_3 is equal to the first normal stress difference N_1. Thus, via the SOR, the first normal stress difference N_1 can be assessed in real time during melt extrusion. This rheo-optical approach was applied to study the hydrolysis and chain extension reactions during reactive processing of PET, and knowing that the stress optical coefficient C is independent of molecular weight[12], one can follow the effects in the first normal stress difference due to changes in the polymer molecular weight.

2. Materials and Methods

2.1 Materials

Polyethylene terephthalate copolymer grade, Cleartuf® Turbo™, with no stabilizers nor additives, donated by M&G Chemicals (Poços de Caldas, MG, Brazil). Pyromellitic dianhydride PMDA, was purchased from Sigma-Aldrich with 97% w/w purity.

2.2 Preparation of water-saturated PET (PETw) and dried PET (PETd)

Pulses made of PETw pellets were used to add a known controlled water amount into the extruder and quantitatively perform the in-line PET hydrolysis measurements: virgin pellets (PETv) were water-saturated in hot water at 90°C; the pellets were air blown at room temperature to remove the externally adsorbed moisture and stored in a bag; the absorbed moisture content of the water-soaked samples was evaluated by gravimetry and DSC. PETd was dried in a Thermolift 100-2 ARBURG dryer (Lossburg, German), with the dry hot air module operating with silica gel at 150ºC. Tests were conducted to set drying time by packing samples in a wire grid and evaluated by gravimetry. In addition, intrinsic viscosity IV and thermal analysis DSC were applied to characterize the PETd.

2.3 Preparation and types of pulse compositions

All in-line measurements were done in the extruder in transient form. A pulse is fed in a steady-state PETd flow: an inert (PETd) and two active pulses (PETw and PMDA) were used to monitor the in-line PET reactions (hydrolysis, chain extension, and both reactions simultaneously). Pulses of 6g and 10g were used in all screw profiles: one of PETd for baseline; second of PETw for in-line hydrolysis monitoring; third of PMDA for chain extension studies; fourth of PETw + PMDA for simultaneous reactions. PMDA was carried in PETd film capsules, with the film prepared by hot-pressing (in a Luxor LPB-35-15 press, LUXOR, São Paulo, Brazil) at 260°C, cut, and folded into 36mm^2 squares envelopes of 0.0010g ± 0.0005g, which were filled with two amounts of PMDA powder (0.050g and 0.030g ± 0.001g) and hot sealed. Four pulses were set, with the number of capsules constant: 0.25g of PMDA (i.e., 5 capsules of 0.050g); 0.25g of PMDA + 10g of PETd; 0.15g of PMDA + 10g of PETd (5 capsules of 0.03g); and 10g of PETw + 0.25g or 0.15g of PMDA.

The pulses were introduced in the extruder feeding hopper by a tubular device, having a scaffold where pulse material is kept (Figure 1a). By sliding sideways the scaffold, the pulse falls into the extruder while the in-line data collection starts to run synchronously. The PETd flowing carries the pulse material downstream, melts, mixture, reactions may occur, and finally, the melt reaches the slit-die at the extruder exit for the in-line optical measurement.

2.4 Twin-screw extruder experimental set-up

The experiments were performed in a co-rotating intermeshing twin-screw extruder Werner & Pfleiderer (W&P) ZSK-30 (30.70mm screw diameter and L/D = 35) with a K-Tron gravimetric feeder. A unique design slit-die has been fitted at the end of the W&P (Figure 1a). It is modular, with two halves separated by two spacers forming a 1.5mm thickness and 15mm width slit. Along its length, it has three pressure transducers and temperature controls. The optical portion has two pairs of borosilicate glass transparent windows (Ø 10 mm; 1 mm thickness) on each side of the slit-die, where an in-line optical detector is docked.

The optical detector has a polarizer filter fixed at 45° relative to the polymer flow direction, polarizing the white light emitted by a LED (λ≈550 mm). The polarized light travels through the melt flowing, reaches another polarizer (set crossed to the first one), and then the photodetector (LDR). LDR quantifies the cross-polarized transmitted light intensity, which is converted in optical path difference (OPD) and finally in birefringence. The LDR and LED are independently adjustable, given a broad range of light intensities that are needed. An analogic-digital interface (USB data acquisition NI-DAQ 6812) collects and converts signals from the LDR into digital signals and transmits them to a PC running software developed in LabView 8.6 NI (National Instruments). It averages data, makes real-time calculations, displays information, and saves data (slit-die temperature, residence time, I_N^c, pressure drop, screw rotation speed and torque). The rheo-optical system was validated by ILT

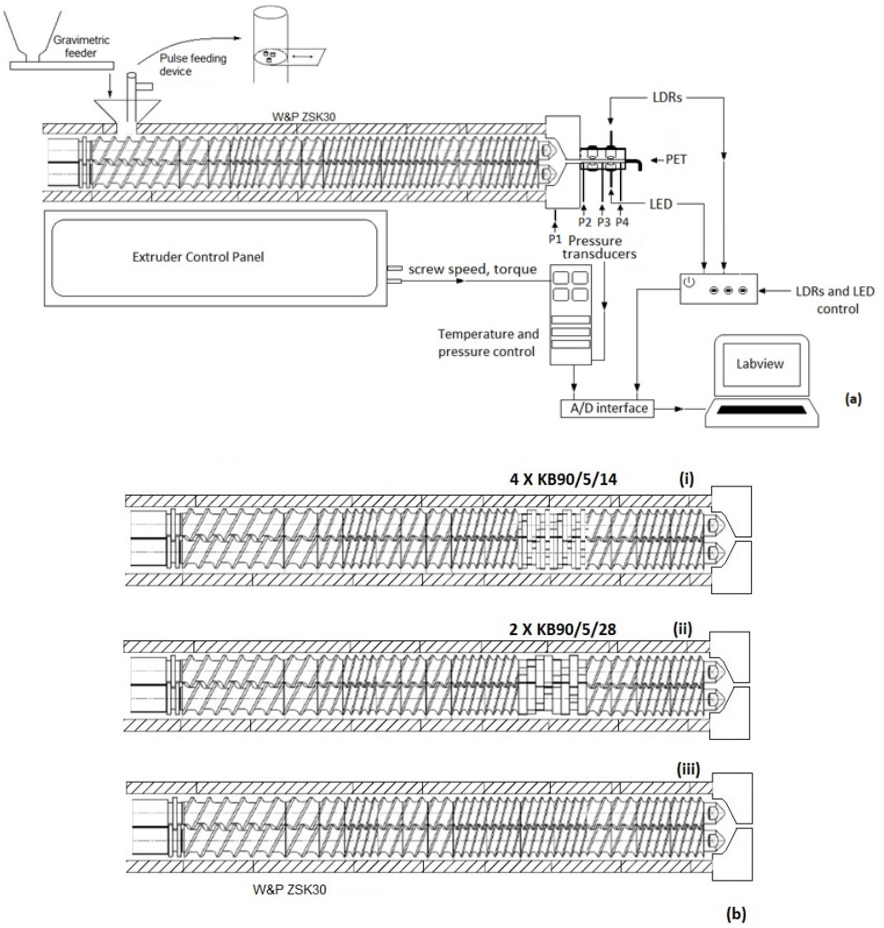

Figure 1. Extruder experimental setup. (a) Slit-die and in-line optical detector system fitted to the extruder, equipped with gravimetric feeders and the tubular scaffold; (b) The three screw profiles used: (i) four KB90-14mm; (ii) two KB90-28mm; (iii) only with conveying elements.

1400 Radiometer/Photometer from Standard International Light Technologies, comparing the response of the two LDRs to a set of fixed luminous intensities emitted by the LED. More information on this slit-die and in-line setup can be found in previous publications[12-14].

Three screw profiles were assembled to evaluate the effect of 90º kneading blocks (KB90) with two different thicknesses. Figure 1b shows them: i) Profile 1, apart from the conveying elements, contains a set of four kneading disc blocks with 90° and 14mm thickness each (KB90-14mm), ii) Profile 2 contains two kneading disc blocks with 90° and 28mm thickness (KB90-28mm). Profile 1 has narrow kneading disks compared to profile 2, which provided a greater mixing capacity with a high level of distributive mixing. iii) Profile 3 is made only of conveying elements, acting as the reference screw profile.

2.5 In-line flow birefringence measured by the rheo-optical detector

During the extrusion in steady state, the melt flow orients in the flow stream, making it possible to measure the total birefringence, which in this study was assumed to be only due to flow birefringence once the PET sample is the same for all experiments, the measurement is done in the melting state, and there is no second phase present. The in-line monitoring evaluates the optical changes in the melt flow, which is oriented at θ = 45° in relation to the pair of crossed polarizers, causing hydrolysis and chain extension, which in turn changes the PET molecular weight. The cross-polarized transmitted light intensity is normalized ( ) as a dimensionless value varying between zero and one as[12,13]:

$$I_N^c = \frac{I - I_c}{I_p - I_c} \tag{3}$$

being I the cross-polarized transmitted light intensity measured during the melt flow experiments, I_c this intensity when the measurement is taken with the pair of polarizing filters set crossed and I_p when the pair is set parallel. Setting the melt flowing at θ = 45° (i.e. the extinction angle) in relation to the pair of crossed polarizers, the Malu's Law reduces to [14]:

$$I_N^c = I_0 \text{sen}^2 2\theta \text{sen}^2 \frac{\delta}{2} = \text{sen}^2 \frac{\delta}{2} \tag{4}$$

Then the normalized intensity I_N^c can be related directly to the optical path difference OPD, and knowing the sample thickness (the slit-die thickness $t = 1500nm$), and assuming the average wave length of white light of $\lambda = 550nm$ one can get the birefringence (Δn)

$$I_N^c = \text{sen}^2\left(\frac{\pi OPD}{\lambda}\right) = \text{sen}^2\left(\frac{\pi \Delta n t}{\lambda}\right) = \text{sen}^2\left(\frac{\pi \Delta n 1500nm}{550nm}\right) \quad (5)$$

2.6 Off-line intrinsic viscosity (IV) measured by glass capillary viscometer

Diluted PET solution intrinsic viscosity, was taken following the ASTM D4603–03 (Standard Test Method for Determining Inherent Viscosity of Poly (Ethylene Terephthalate) (PET) by Glass Capillary Viscometer) procedure, using the Billmeyer equation[15]:

$$[\eta] = \frac{0.25(\eta_r - 1 + 3\ln\eta_r)}{C} \quad (6)$$

being η_r the relative viscosity (t / t_o), t average solution flow time, average solvent flow time and C polymer solution concentration in g/dL. Knowing the IV, the polymer viscosity average molecular weight ($\overline{M_v}$) can be estimated using the Mark-Houwink-Sakurada equation[15]:

$$[\eta] = K\left(\overline{M_v}\right)^a \quad (7)$$

being [η] the IV, a and K constants which for PET in phenol/1,1,2,2-tetrachloroethane solution, 60/40 weight %, are a=0.68 and K=7.44x10^{-4}dL/g[16].

2.7 PET thermal characterization by DSC

Thermal characterization was done in a Differential Scanning Calorimeter DSC (TA Instruments, Q2000) calibrated with indium standard (Tm=155.6°C, ΔH=6.8 cal/g, at 10°C min^{-1}). Thermo-cycle protocol used was the heating rate at 10°C/min from room temperature to 320°C for PETw and PETd and to 370ºC for PMDA, with all samples weighing from 6 to 7mg.

3. Results and Discussions

3.1 Off-line characterization of PETv, PETd, PETw and PMDA

PETv and PETd samples showed the same 0.7dl/g IV. The kinetics of the PET hydrolysis reaction is slow up to 180°C but increases fast at higher extrusion temperatures[3,17]. Thus, PET will undergo a quick and intense reaction with the absorbed water during extrusion, causing chain scission, which reduces its molecular weight and consequently drops its IV. PETv sample showed 0.35 wt% initial moisture content and was divided into two batches: one to be dried and the other to be water-saturated. Both methods were tested to get the best time for each process. The drying process at 150ºC needed 4h to remove 0.4 wt% of moisture, close to the value presented by PETv. The water saturation process took a soaking time of 72h at 90ºC to reach the equilibrium moisture absorption of 0.86 wt%. Figure 2a and b show these results.

DSC data show that the water absorbed present in PETw shifts both glass transition (Tg) and melting temperatures (Tm) to a lower value than PETd (Figure 3a). Water molecules set in the hydrogen bonds, formed among ester groups in the amorphous phase, reducing their bond energy. It eases the relative movement among adjacent molecules, acting as chain lubricant, thus reducing its Tg. At higher temperatures, the thermo-activated degradation process of hydrolysis takes over, creating chain scission, reducing chain length, and increasing chain mobility. The crystalline micelle size is reduced, and thus their Tm. This effect occurred due to scission in chain segments within crystalline/amorphous diffuse interface.

The PMDA DSC curve, Figure 3b, shows a narrow melting peak at 290 °C and another small melting peak at 240ºC, which may be due to impurities. Note that the heat flow full scale of the PMDA DSC curve is 5x greater than PETw and PETd DSC curves.

3.2 PET flow birefringence in-line characterization during steady-state extrusion

PET processability was tested by running the extruder at four temperatures 245, 255, 265, and 275°C, maintaining a constant temperature profile along the barrel, feeding rate (3Kg/h), screw rotation speed (100 rpm), and screw profile 1 (KB90, 14mm). The average flow birefringence, as normalized cross-polarized transmitted light intensity, was measured in steady-state by the rheo-optical detector. Flow birefringence is highest at the lowest barrel temperature of 245°C (Δn = 0,033) decreasing as extrusion temperature increases (at 255ºC Δn = 0,0293, at 265ºC Δn = 0,0271, at 275ºC Δn = 0,0277) implying a reduction in flow orientation, caused mainly by the reduction of their relaxation time. Other thermo-mechanical degradation processes may also reduce PET molecular weight but are not considered here.

3.3 PET flow birefringence in-line characterization during transient-state extrusion

Pulses containing a fixed amount of chain extender (e.g., 0.25g PMDA + 10g of PETd) were introduced into a steady-state flow of PETd using the same processing conditions described in the previous section. Figure 4a shows the RTD curves at 4 different extrusion temperatures, which run from ~100s up to ~400s. An RTD curve is obtained if the introduced pulse produces changes in the downstream melt flow, which can be detected by the in-line detector. Here, the PETd component of the pulse and the PMDA itself does not produce any detectable effect. Yet, the PMDA extrusion process with PET melt flow causes a chain extension reaction, increasing PET molecular weight and so the flow orientation, while passing by the slit-die. This change alters the PET melt flow birefringence, which is sensed by the in-line rheo-optical detector as normalized cross-polarized transmitted light intensity I_N^c. In Figure 4a, all curves were normalized by their baseline curves at each temperature. Direct comparison can only be made if the OPD induced by the oriented flow is lower than 275nm, i.e., still inside the first half of the first order in Michel

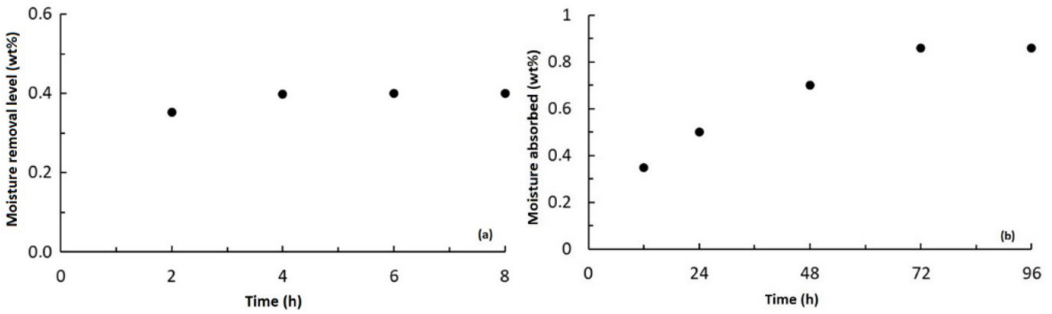

Figure 2. (a) Moisture removal from PETv during the drying process at 150ºC at different times to evaluate the best set-up to produce the dry PETd; (b) PETv moisture absorbed in the water saturation process, soaked at 90°C, to prepare the wet PETw.

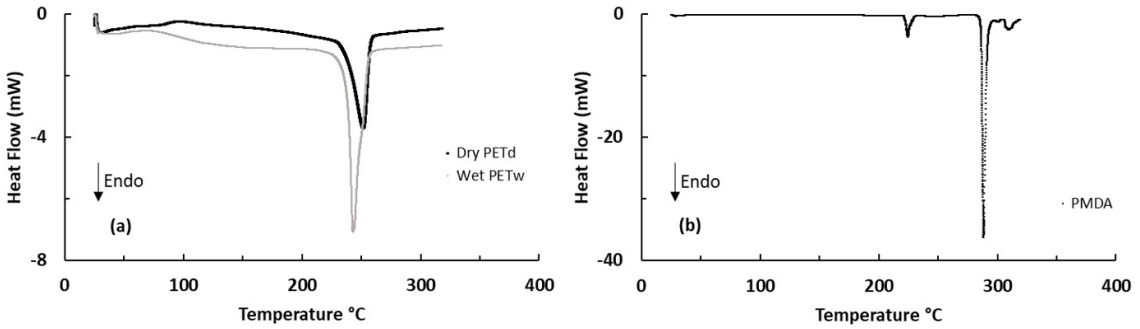

Figure 3. DSC of (a) PETd and PETw and (b) PMDA at a heating rate of 10°C/min.

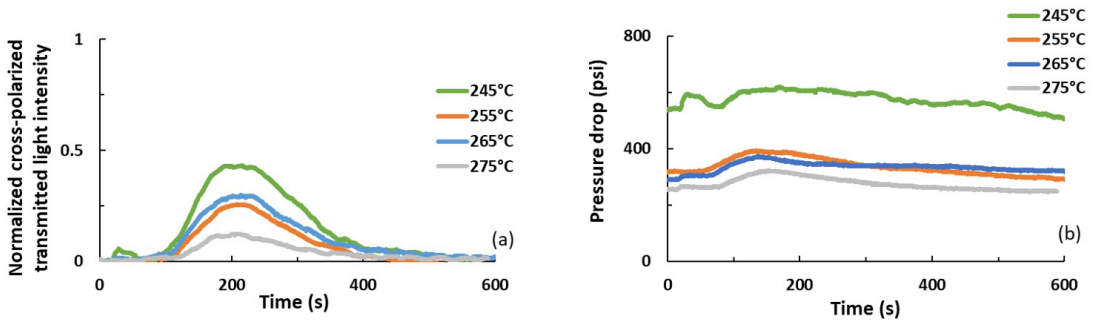

Figure 4. In-line optical monitoring of 10g PETd + 0.25g PMDA pulse during PET extrusion at different temperatures. (a) normalized cross-polarized transmitted light intensity (I_N^c); (b) slit pressure drop. Processing condition: screw profile 1 (KB90, 14mm); 3Kg/h; 100rpm.

Levy's chart. This optical condition can be experimentally set by properly adjusting the slit-die thickness – the reason why the die was designed having two halves, separated by a replaceable spacer, which sets the suitable slit thickness.

RTD curves can be visualized from 245°C to 275°C barrel temperatures, all below the PMDA melt temperature (290ºC from DSC), indicating that PMDA/PET chain extension reaction occurred, even at temperatures as low as 245ºC. One possible explanation is that PMDA melted in the screw kneading zone, due to PET chains Plastic Energy Dissipation[18], responsible for a melt PET flow temperature increase in short times. After passing by the high shear kneading zone the PET/PMDA melt temperature is brought back to the set barrel temperature. Another contribution is heat generation from the viscous heating occurring due to the large strain rates undergone in extrusion. Heat generation is proportional to PET viscosity, which, is overcome by its dependency squared on strain rate square. Thus, PET-flow carrying PMDA reaches temperatures higher than the set barrel temperature, melting PMDA. A detectable RTD curve indicates that these effects are contributing to the melting of the PMDA.

Figure 4b shows the pressure drop, along the slit-die, in the RTD detection region. The pressure drop increases slightly, indicating a slight rise in the melt flow viscosity due to chain extension. The increase in the pressure drops, measured at RTD curves' peak, is kept almost constant, regardless the extrusion temperature. The results suggest the reaction is occurring during extrusion, as expected, and nearly to the same extent in all temperatures tested.

3.4 PET hydrolysis in-line characterization during transient-state extrusion

In-line birefringence and pressure drop measurements were used to monitor the transient-state PET hydrolysis during extrusion in three different screw profiles (see Figure 1b). Figure 5a shows the in-line I_N^c (as in-line flow birefringence), and (b) the pressure drop in the slit-die, measured using the processing condition: 3 kg/h, 100 rpm, and 245 ºC for screw profile 1. The procedure started by introducing PETd pulses in PETd flow to set the baseline curve. The I_N^c curve remains close to zero, indicating no flow birefringence, and the pressure drop remains constant at 600 psi. In both cases, no sign of an RTD curve is shown, indicating that introducing a dry PET pulse into the flow it does not change the flowing orientation of the polymer and so the shear rate, thus the PET average molecular weight remains constant. On the other hand, when pulses of wet PET (PETw) are introduced, I_N^c curves (as flow birefringence) and pressure drop curves show an "upside-down" RTD curve, producing data below their baseline, indicating a reduction of flow orientation and a decrease in viscosity. Hydrolysis causes the scission of ester bonds in the PET chains, decreasing the molecular weight and thus its melt viscosity. As expected, raising the weight content of PETw on the pulse intensifies the hydrolysis level (10g PETw pulse has 0.086g water compared to 6g PETw pulse holding 0.052g water).

Peaks at the beginning of the RTD curves, seen in Figures 4 and 5, were observed at about ~15 s. By monitoring the extruder torque, we could conclude that the sudden pellet mass increases while the pulse is fed creates a short and reversible mechanical disturbance, with no consequence to the RTD curve, which starts later at ~100s.

During the screw profile design, kneading elements were added to intensify shearing of the melt flow, improving the mixing performance during extrusion. Three screw profiles (Figure 1 b) were used to evaluate their effects in the PET hydrolysis. Figure 6 shows the "upside-down" RTD curves when introducing wet PETw pulses. Comparing the three RTD curves produced by the three screw profiles, the presence and type of kneading disc blocks affect the hydrolysis level. Screw profile 1 with narrow KB90, produces the highest drop. Screw profile 2 shows an intermediate effect with wide KB90. Finally, screw profile 3, having only conveying elements, indicates the lowest effect. Also, screw profiles 1 and 2 have longer residence times, increasing the time for the reaction to occur inside the extruder. The set of KB90 had an equal total length of the kneading zone, differing in the thickness of the disks; narrow disks produce a more intense distributive mixture, causing a more effective hydrolysis.

Table 1 shows the lowest flow birefringence values calculated using equations presented in section 2.7, by using the lowest value of the I_N^c reached in each curve, compared to baseline. The lowest flow birefringence, 11.1×10^{-3}, was achieved when introducing 10g of wet PETw pulse in profile 1, in contrast to 33.4×10^{-3} from adding dry PETd, a reduction of 22.3×10^{-3}. A similar effect, but smaller, was observed for profiles 2 and 3. A longer residence time and greater shear mixing level provided by profile 1 were sufficient to induce the hydrolysis reaction decreasing the molecular weight and melting viscosity.

3.5 PET chain extension in-line characterization during transient-state extrusion

The PET chain extension using PMDA was monitored in-line by measuring flow birefringence (as I_N^c) and pressure drop along the slit-die. Pulses made of PETd/PMDA were introduced in the melt flow of PETd (conditions in Figure 7). This reaction ties together two or more PET chains producing

Table 1. Effect of the screw profiles in the hydrolysis of PET melt flow during extrusion, as flow birefringence, measured at the minimum of the RTD curve.

Screw profile/Flow birefringence	Pulse of 10g PETw	Pulse of 6g PETw
Profile 1 (KB90, 14mm)	11.1×10^{-3}	14.3×10^{-3}
Profile 2 (KB90, 28mm)	14.1×10^{-3}	14.6×10^{-3}
Profile 3 (only conveying)	19.6×10^{-3}	18.5×10^{-3}

Flow birefringence of dry PETd = 33.4×10^{-3} (from section 3.2)

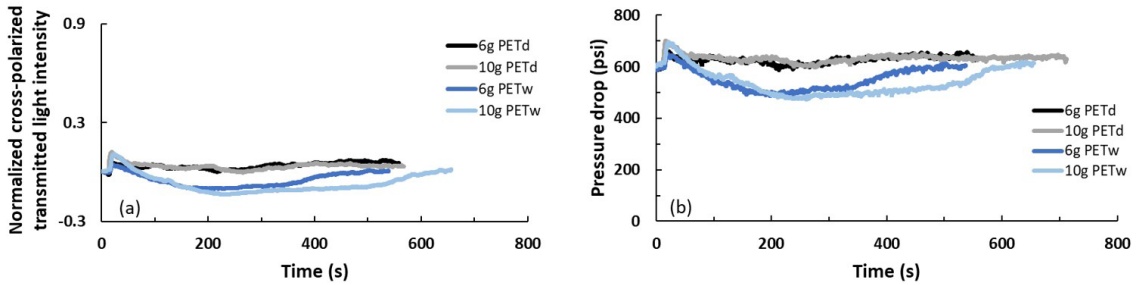

Figure 5. In-line optical monitored the effect of adding PETd and PETw pulses to a steady-state extrusion melt flow of PETd: (a) normalized cross-polarized transmitted light intensity and; (b) pressure drop curves. Screw profile 1 (KB90, 14mm), 3Kg/h, 100rpm and 245°C.

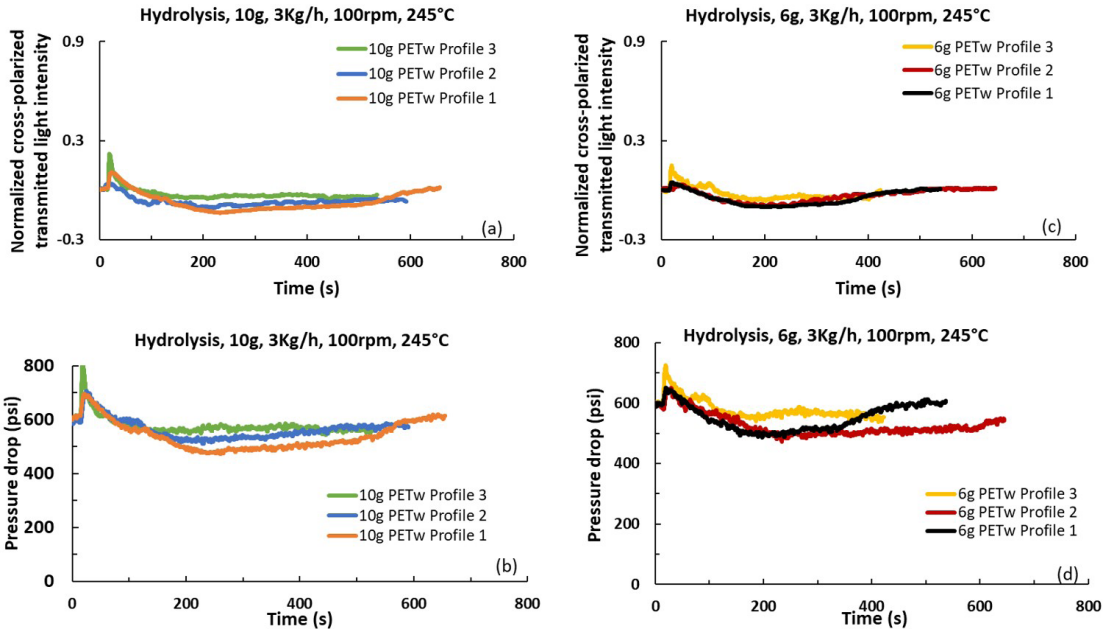

Figure 6. In-line monitoring PET hydrolysis using three different screw profiles, screw profiles 1 (KB90, 14mm), profile 2 (KB90, 28mm), and profile 3 (only conveying): (a) and (c) normalized cross-polarized transmitted light intensity, (b) and (d) pressure drop curves.

longer molecules and increasing PET average molecular weight; melt viscosity; chain relaxation time; flow orientation; and, as a result, an increase in flow birefringence (as I_N^c), seen in the RTD curves. Turbidity was also measured while the experiments were running (not shown), but no RTD curve was detected, denoting that the PMDA was not dispersed as fine particles that would scatter light, but rather molten and well mixed in the PET melt.

Figure 7 shows RTD curves obtained with different amounts of PMDA. The I_N^c rises above the baseline, denoting an increase in the flow orientation, i.e., confirming the PET chain extension reaction. The curve made by the pulse having only 0.25g PMDA reaches the highest value, followed by a pulse made of 0.25g PMDA + 10g of PETd, and the third, formed by a pulse of 0.15g PMDA + 10g of PETd, shows the lower intensity. The two pulses having the same PMDA amount differ because the extra amount of dry PETd dilutes the PMDA, reducing the reacted chain content in the melt.

Figure 8 shows in-line birefringence, as I_N^c, and pressure drop RTD curves. The amount of PMDA in the pulses affects the size of the RTD curve, and likewise, the more shearing the screw profile is, the greater the RTD curve, indicating a higher chain extension reaction. This behavior is seen in the most shearing profiles 1 and 2, even though the data are somehow overlapped. A dispersive mixture imparted by the KB90 favored the chain extension reaction. The pressure drop measurements follow the same pattern but are much less sensitive, with data more scattered. As the reacted polymer flow passes by the slit-die, the pressure drop increases, showing that the molecular weight of the PET increases, which confirms the extension reaction.

Table 2 shows the highest value of PET flow birefringence calculated from the I_N^c value measured at the RTD curves

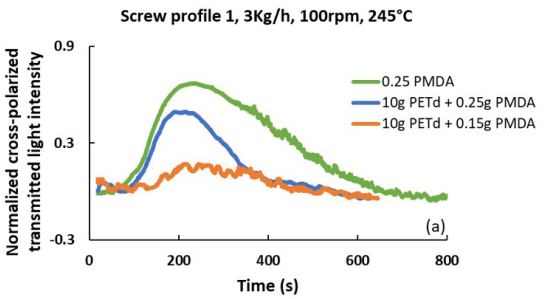

Figure 7. RTD curves measured during chain extension analysis in transient-state by in-line normalized cross-polarized transmitted light intensity $\left(I_N^c\right)$ in screw profile 1, [KB90, 14mm].

maximum. For comparison, using as a baseline the value of PETd as 33.4x10-3(see section 3.2). Profiles 1 and 2, with KB90, presented a higher increase in the flow birefringence, reaching 90x10-3 for the 0.25g PMDA pulse, 80x10-3 for the 0.25g PMDA + 10g PETd pulse and 59x10-3 for the 0.15g PMDA + 10g PETd pulse.

3.6 Simultaneous PET hydrolysis and chain extension in-line characterization

The simultaneous addition of wet PETw and PMDA during in-line monitoring allows analyzing the two opposite reactions, hydrolysis, and chain extension, shown in Figure 9.

The in-line birefringence and pressure drop curves were obtained with pulses with 0.25g PMDA + 10g PETw and 0.15g PMDA + 10g PETw. The reagent molecule number in the first case is almost equal, taking each reaction

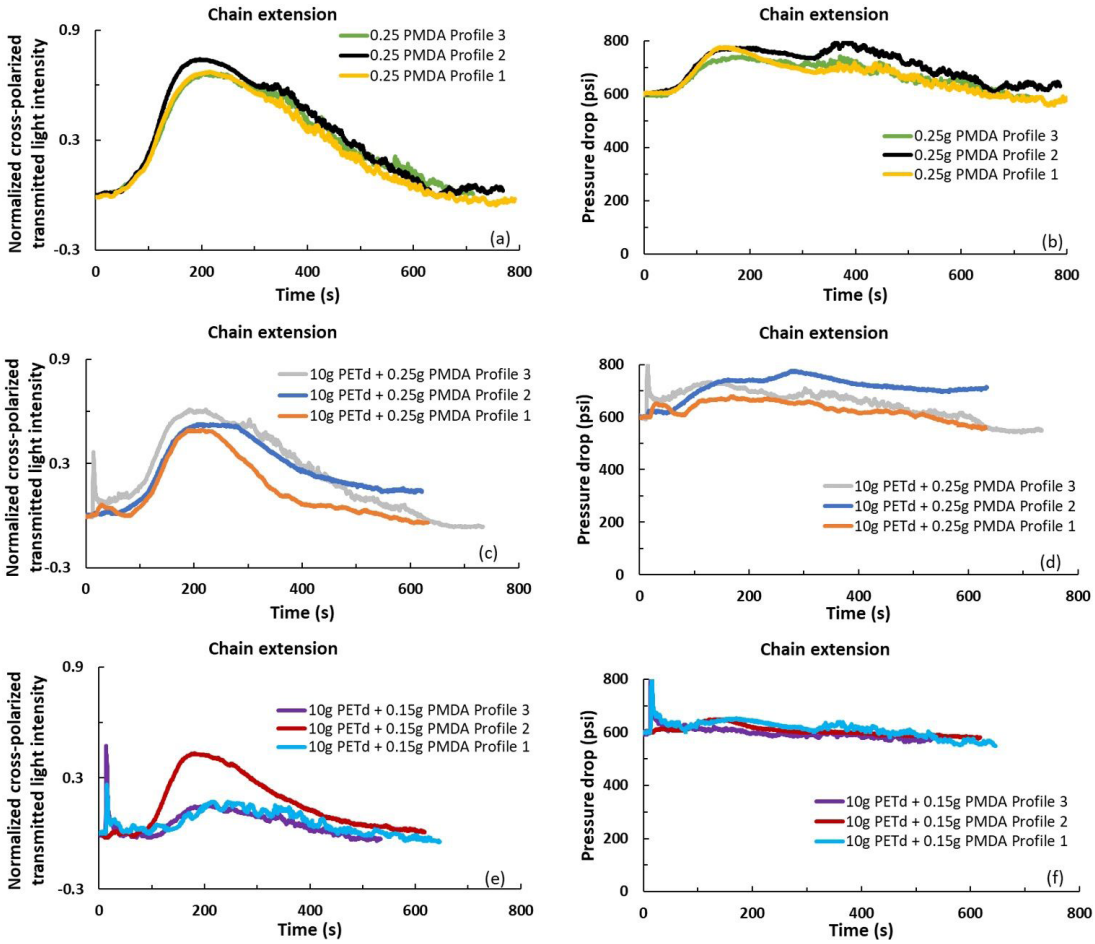

Figure 8. Effect of KB90 elements in the PET chain extension reaction, measured in-line. In (a), (c) and (e) is plotted flow birefringence curves (as I_N^c), and in (b), (d) and (f) pressure drop curves. Extrusion processing conditions: 245°C, 3Kg/h and 100rpm. Screw profile 1 (KB90, 14mm), profile 2 (KB90, 28mm), and profile 3 (only conveying).

Table 2. Effect of the screw profiles in the chain extension reaction with PMDA.

Screw profile/Flow birefringence	Pulse of (0.25g PMDA)	Pulse of (0.25g PMDA + 10g PETd)	Pulse of (0.15g PMDA + 10g PETd)
Profile 1 (KB90, 14mm)	89.5×10^{-3}	78.9×10^{-3}	58.3×10^{-3}
Profile 2 (KB90, 28mm)	94.0×10^{-3}	80.8×10^{-3}	75.3×10^{-3}
Profile 3 (only conveying)	88.9×10^{-3}	85.8×10^{-3}	57.0×10^{-3}

Flow birefringence of PETd = 33.4×10^{-3}.

stoichiometry, 1:1 for the hydrolysis and 1:4 for the chain extension reactions (PMDA is tetra-functional). A pulse with 0.25g PMDA has 0.9 mmol of PMDA, and 10g PETw holds 4.8 mmol of water, 5 times higher, compensating for the difference in stoichiometry. Figure 9 shows two RTD curves superposition, shifted in time. The pulse release with the two components was simultaneous. Their reaction occurred downstream but shifted in time. The upside-down RTD curve, hydrolysis, occurs first. Later, the chain extension leads the reaction, creating a regular shape RTD curve. As the water is present in the PETw pulse it reacts in the polymer, hydrolysis can start after entering the extruder and continue as the polymer gets heated. Some water molecules may vaporize, escaping from the melt and diffusing forward following the partially filled screw channels and reacting with other PET chains at the flow downstream. These hydrolyzed chains reach the extruder exit (and so are detected) first, making up the initial part of the RTD curve. The PMDA powder in the envelopes needs to be heated to melt and then start to react with the PET chains, retarding the reaction along the screw length. Also, the forward movement imposed by the screw to the PMDA envelopes, which are bigger than the PET pellets, is less efficient than the one transferred to the molten PET stream, retarding them. Thus, the extended chains take longer to reach the detector, forming the second part of the RTD curves. The same behavior is presented by

Table 3. In-line flow birefringence during simultaneous hydrolysis and chain extension reactions. Effect of pulse content and screw profile.

Screw profile/Flow birefringence (PETd = $33.4x10^{-3}$)	Pulse of (0.25g PMDA + 10g PETw)		Pulse of (0.15g PMDA + 10g PETw)	
	Min	Max	Min	Max
Profile 1 (KB90, 14mm)	$21x10^{-3}$	$55x10^{-3}$	$21x10^{-3}$	$43x10^{-3}$
Profile 2 (KB90, 28mm)	$15x10^{-3}$	$57x10^{-3}$	$16x10^{-3}$	$45x10^{-3}$
Profile 3 (only conveying)	$17x10^{-3}$	$54x10^{-3}$	$16x10^{-3}$	$24x10^{-3}$

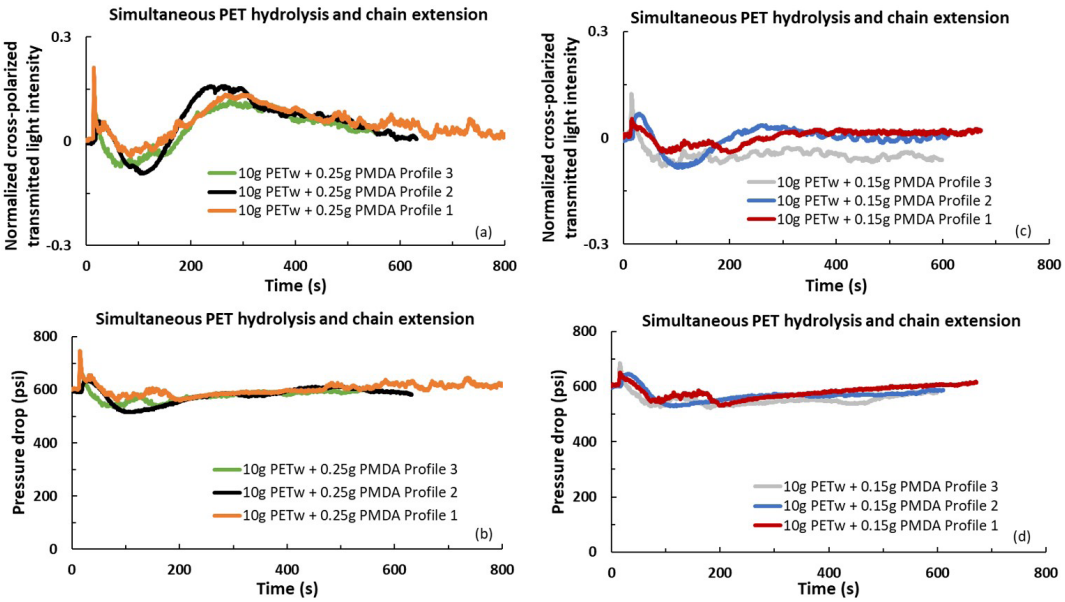

Figure 9. In-line monitoring of simultaneous hydrolysis and chain extension during PET extrusion, using screw profiles 1 (KB90, 14mm), profile 2 (KB90, 28mm), and profile 3 (only conveying). Pulse contents as PETw and PMDA and screw profile type used are shown at each legend box of a) to d) plots. Extrusion processing conditions: 245°C, 3Kg/h and 100rpm.

pressure drop graphs, seen in Figures 9c and d, showing the two shifted curves.

Table 3 presents the minimum and maximum values of PET flow birefringence attained by each pulse in the three screw profiles. The higher the PMDA content in the pulse, the higher the conversion of the chain extension reaction, the higher the flow birefringence.

3.7 PET off-line characterization

During in-line monitoring, polymer melt samples were collected at the extrusion exit, at the maximum of the RTD curve. They were characterized off-line by measuring their IV, which provides $\overline{M_v}$ by using Mark-Houwink-Sakurada equation[15], with results shown in Table 4. PETv has 0.7dl/g IV, indicating a $\overline{M_v} = 38,000$. When PETd pulse was added, IV dropped to $0.6 dl/g$, indicating a $\overline{M_v} = 28,000$. The addition of PETw pulses reduced the IV to 0.5dl/g ($\overline{M_v} = 23,000$), and PMDA pulses increases back to 0.64dl/g ($\overline{M_v} = 33,000$). The IV values are dependent on the screw profiles, indicating a higher chain extension reaction in profile 2 and hydrolysis reaction in profile 1. Profile 3, the mildest, induces lower conversion rates in both reactions. These off-line values corroborate the in-line flow birefringence measured in the previous sections, confirming the efficacy of the proposed in-line rheo-optical detection method.

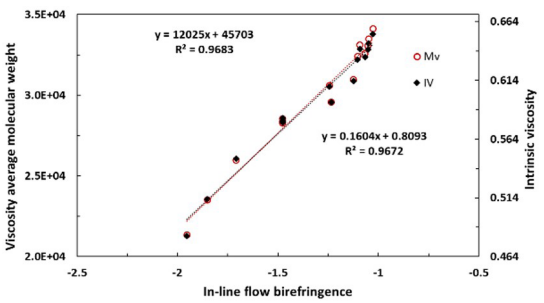

Figure 10. PET $\overline{M_v}$ and IV as a function of in-line flow birefringence, for all samples tested. The linear fitting equations and accuracies are indicated, showing good agreement between in-line flow birefringence (in log scale) and off-line Mv and IV (in linear scale) measurements.

To quantitatively evaluate how accurate in-line measurements are compared to off-line data, in-line flow birefringence was plotted as a function of intrinsic viscosity and *Mv*. Figure 10 shows this correlation as a straight line with excellent fittings. The intrinsic viscosity relation comes as $IV = 0.160 \times \log \Delta n + 0.81$ (R2 = 0.97) and $Mv = 12025 \times \log \Delta n + 45703$ (R2 = 0.97). These relations are

Table 4. In-line flow birefringence (Δn), off-line IV, and calculated $\overline{\ }$, of PET samples collected during extrusion, at the maximum of the RTD curve.

PETv IV = 0.7dl/g $\overline{M_v}$ = 38,000			Pulse components and content				
			10g PETd	10g PETw	0.25g PMDA	10g PETd + 0.25g PMDA	10g PETd + 0.15g PMDA
Melt processed PET properties	Δn (x10^{-3})	Profile 1	33.4	11.1	89.5	78.9	58.3
		Profile 2	33.4	14.1	94.0	80.8	75.3
		Profile 3	33.4	19.6	88.9	85.8	57.0
	IV (dl/g)	Profile 1	0.579	0.482	0.645	0.632	0.595
		Profile 2	0.578	0.513	0.653	0.641	0.613
		Profile 3	0.582	0.547	0.640	0.634	0.609
	$\overline{M_v}$	Profile 1	28,400	21,300	33,500	32,400	29,600
		Profile 2	28,300	23,500	34,100	33,100	31,000
		Profile 3	28,500	26,000	33,100	32,600	31,000

valid for a twin-screw extruder with L/D = 35, processing PET at 245 °C, 3Kg/h and 100 rpm. This knowledge may be used in the development of quality control during industrial PET extrusion processes and real-time quantification during PET recycling.

4. Conclusions

During twin-screw extrusion of PET, reactions of hydrolysis and chain extension were induced by adding reactant pulses in the melt flow and quantified via in-line rheo-optical measurements. The melt elasticity was followed by measuring flow birefringence and pressure drop along a slit-die, done by a rheo-optical detector. The results come as residence time distribution RTD curves, with unique forms: with its maximum value pointing upwards when the melt elasticity increases, as is the case of chain extension, or an RTD curve upside down, pointing downwards, when the reaction is by chain scission. PET hydrolysis and chain extension depend on the type and content of the active agent. They also depend on the melt shearing type and level imposed by the extruder screw profile. Hydrolysis is more effective when screw profiles having narrow KB90 are used, inducing preferential distributive mixing, while chain extension is more sensitive to wide KB90, which has a preferential dispersive mixing character. Off-line measurements of intrinsic viscosity (IV) and its corresponding molecular weight ($\overline{M_v}$) corroborate the in-line measurements. By assuming collinearity and full birefringence orientation along the melt flow direction the flow birefringence, measured in the 2-direction (Δn_{12}), can be used to monitored in-line the elasticity of the melt, taken as first normal stress difference (N_1), which in turn is affected by changes in the polymer melt molecular weight. The proposed real-time rheo-optical technique was successfully applied to follow chain extension and hydrolysis reactions occurring during PET melt extrusion.

5. Author's Contribution

- **Conceptualization** – Luciana Assumpção Bicalho; Sebastião Vicente Canevarolo Junior.
- **Data curation** – Luciana Assumpção Bicalho; Sebastião Vicente Canevarolo Junior.
- **Formal analysis** – Luciana Assumpção Bicalho; Sebastião Vicente Canevarolo Junior.
- **Funding acquisition** – Sebastião Vicente Canevarolo Junior.
- **Investigation** – Luciana Assumpção Bicalho; Sebastião Vicente Canevarolo Junior.
- **Methodology** – Luciana Assumpção Bicalho; Sebastião Vicente Canevarolo Junior.
- **Project administration** –Sebastião Vicente Canevarolo Junior.
- **Resources** – Luciana Assumpção Bicalho; Sebastião Vicente Canevarolo Junior.
- **Software** – Luciana Assumpção Bicalho; Sebastião Vicente Canevarolo Junior.
- **Supervision** – Sebastião Vicente Canevarolo Junior.
- **Validation** – Luciana Assumpção Bicalho; Sebastião Vicente Canevarolo Junior.
- **Visualization** – Luciana Assumpção Bicalho; Sebastião Vicente Canevarolo Junior.
- **Writing – original draft** – Luciana Assumpção Bicalho; Sebastião Vicente Canevarolo Junior.
- **Writing – review & editing** – Luciana Assumpção Bicalho; Sebastião Vicente Canevarolo Junior.

6. Acknowledgments

This study was financed by the Coordenação de Aperfeiçoamento de Pessoal de Nível Superior - Brasil (CAPES) - Finance Code 001, PROEX 88882.332717/2019-01 scholarship to L.A. Bicalho, and Conselho Nacional de Desenvolvimento Científico e Tecnológico (CNPq) for a PQ scholarship 311790/2013-5 to S.V. Canevarolo, and the Programa de Pós-Graduação em Ciência e Engenharia de Materiais (PPG-CEM) of UFSCar.

7. References

1. Awaja, F., & Pavel, D. (2005). Recycling of PET. *European Polymer Journal*, *41*(7), 1453-1477. http://dx.doi.org/10.1016/j.eurpolymj.2005.02.005.
2. Scheirs, J. (2004). *Additives for the modification of poly(ethylene terephthalate) to produce engineering-grade polymers.* In J.

Scheirs, & T. Long (Eds.), *Modern polyesters: chemistry and technology of polyesters and copolyesters* (pp. 495-540). England: John Wiley & Sons, Ltd. http://dx.doi.org/10.1002/0470090685.ch14.

3. Campanelli, J. R., Kamal, M. R., & Cooper, D. G. (1993). A kinetic study of the hydrolytic degradation of polyethylene terephthalate at high temperatures. *Journal of Applied Polymer Science*, *48*(3), 443-451. http://dx.doi.org/10.1002/app.1993.070480309.
4. Kao, C.-Y., Wan, B.-Z., & Cheng, W.-H. (1998). Kinetics of hydrolytic depolymerization of melt poly (ethylene terephthalate). *Industrial & Engineering Chemistry Research*, *37*(4), 1228-1234. http://dx.doi.org/10.1021/ie970543q.
5. Pirzadeh, E., Zadhoush, A., & Haghighat, M. (2007). Hydrolytic and thermal degradation of PET fibers and PET granule: the effects of crystallization, temperature, and humidity. *Journal of Applied Polymer Science*, *106*(3), 1544-1549. http://dx.doi.org/10.1002/app.26788.
6. Hosseini, S. S., Taheri, S., Zadhoush, A., & Mehrabani-Zeinabad, A. (2007). Hydrolytic degradation of poly (ethylene terephthalate). *Journal of Applied Polymer Science*, *103*(4), 2304-2309. http://dx.doi.org/10.1002/app.24142.
7. Awaja, F., Daver, F., & Kosior, E. (2004). Recycled poly (ethylene terephthalate) chain extension by a reactive extrusion process. *Polymer Engineering and Science*, *44*(8), 1579-1587. http://dx.doi.org/10.1002/pen.20155.
8. Incarnato, L., Scarfato, P., Di Maio, L., & Acierno, D. (2000). Structure and rheology of recycled PET modified by reactive extrusion. *Polymer*, *41*(18), 6825-6831. http://dx.doi.org/10.1016/S0032-3861(00)00032-X.
9. Covas, J. A., Nóbrega, J. M., & Maia, J. M. (2000). Rheological measurements along an extruder with an on-line capillary rheometer. *Polymer Testing*, *19*(2), 165-176. http://dx.doi.org/10.1016/S0142-9418(98)00086-5.
10. Silva, J., Santos, A. C., & Canevarolo, S. V. (2015). In-line monitoring flow in an extruder die by rheo-optics. *Polymer Testing*, *41*, 63-72. http://dx.doi.org/10.1016/j.polymertesting.2014.10.007.
11. Muller, R., & Vergnes, B. (1996). Validity of the stress optical law and application of birefringence to polymer complex flows. *Rheology Series*, *5*, 257-284. http://dx.doi.org/10.1016/S0169-3107(96)80010-4.
12. Janeschitz-Kriegl, H. (1969). *Flow birefringence of elastico-viscous polymer systems.* In: F. der Hochpolymeren-Forschung. *Advances in polymer science* (pp. 170-318). Germany: Springer Berlin Heidelberg. http://dx.doi.org/10.1007/BFb0051073.
13. Soares, K., Santos, A. M. C., & Canevarolo, S. V. (2011). In-line rheo-polarimetry: a method to measure in real time the flow birefringence during polymer extrusion. *Polymer Testing*, *30*(8), 848-855. http://dx.doi.org/10.1016/j.polymertesting.2011.08.007.
14. Wódkiewicz, K. (1995). Classical and quantum Malus laws. *Physical Review. A, Atomic, Molecular, and Optical Physics*, *51*(4), 2785-2788. http://dx.doi.org/10.1103/PhysRevA.51.2785. PMid:9911909.
15. Billmeyer, F. W., Jr, & Stockmayer, W. H. (1950). Method of measuring molecular weight distribution. *Journal of Polymer Science*, *5*(1), 121-137. http://dx.doi.org/10.1002/pol.1950.120050106.
16. Van Krevelen, D. W., & Te Nijenhuis, K. (2009). *Properties of polymers: their correlation with chemical structure; their numerical estimation and prediction from additive group contributions*. Netherlands: Elsevier. http://dx.doi.org/10.1016/B978-0-08-054819-7.00001-7.
17. Odian, G. (2004). *Principles of polymerization*. USA: John Wiley & Sons, Inc.. http://dx.doi.org/10.1002/047147875X.
18. Qian, B., & Gogos, C. G. (2000). The importance of plastic energy dissipation (PED) to the heating and melting of polymer particulates in intermeshing co-rotating twin-screw extruders. *Advances in Polymer Technology*, *19*(4), 287-299. http://dx.doi.org/10.1002/1098-2329(200024)19:4<287::AID-ADV5>3.0.CO;2-K.

Received: Aug. 04, 2022
Revised: Apr. 23, 2023
Accepted: May 19, 2023